Kelvin Wave Variability in the Upper Stratosphere Observed in SBUV Ozone Data

WILLIAM J. RANDEL AND JOHN C. GILLE

National Center for Atmospheric Research, Boulder, Colorado*

(Manuscript received 15 November 1990, in final form 18 April 1991)

ABSTRACT

The signatures of equatorially trapped Kelvin waves in the upper stratosphere are analyzed in Solar Backscatter Ultraviolet (SBUV) ozone data over the years 1979–86. Comparisons are first made with contemporaneous Limb Infrared Monitor of the Stratosphere (LIMS) ozone data to validate the SBUV Kelvin wave signatures. SBUV and LIMS data both show coherent Kelvin wave oscillations in the upper stratosphere, where ozone is photochemically controlled, and mirrors the temperature fluctuations associated with Kelvin waves; however, SBUV data underestimate wave amplitudes by 20%–60%. Furthermore, transport-induced Kelvin wave patterns in the lower stratosphere are not observed in SBUV data. The eight years of SBUV data reveal the regular occurrence of eastward-propagating zonal wave 1–2 Kelvin waves with periods in the range of 5–15 days. These data show a strong semiannual modulation of Kelvin wave activity, as documented previously in rocketsonde observations. Eight-year-average ensemble spectra are compared to the semiannual oscillation (SAO) in stratospheric zonal winds; a seasonal asymmetry in the strength of Kelvin waves is found, which mimics that observed in the zonal winds. There is a near exact phasing of maxima in wave variance with the strongest easterly zonal winds, i.e., when the wind acceleration is near zero; this argues that Kelvin waves are not a determining factor in the westerly acceleration phase. An exception is found near the stratopause in January when Kelvin wave maxima coincide with strong westerly acceleration. Interannual variability of Kelvin waves is studied in relation to that of the stratospheric zonal winds. No consistent relationship with the quasi-biennial oscillation (QBO) in the lower stratosphere is observed, and correlations with upper stratospheric winds are weak or nonexistent.

1. Introduction

A significant fraction of the variance in stratospheric zonal-wind and temperature fields in the tropics is observed to occur in the form of equatorially trapped, eastward-propagating planetary wave oscillations termed Kelvin waves. Analyses of meteorological rocket and satellite data have revealed Kelvin waves in the upper stratosphere with periods near 5–10 days and vertical wavelengths in the range 10–40 km (Hirota 1978, 1979; Salby et al. 1984). Kelvin waves identified in the lower stratosphere are peaked at somewhat longer periods (10–15 days) and shorter vertical wavelengths (5–15 km) (Wallace and Kousky 1968; Angel et al. 1973). The absorption of vertically propagating Kelvin waves provides a source of westerly momentum in the equatorial stratosphere; in particular, they likely play an important role in the quasi-biennial oscillation (QBO) of the zonal mean wind in the lower stratosphere (Holton and Lindzen 1972). They also possibly contribute to the westerly acceleration phase of the semiannual oscillation (SAO) at the stratopause (Dunkerton 1979), although Hitchman and Leovy (1988) and Hamilton and Mahlman (1988) suggest that internal gravity waves are also important (or dominant).

The signature of Kelvin waves is also observed in satellite observations of stratospheric ozone (and other trace constituents) over the equator (Randel 1990). These ozone Kelvin waves are produced by two distinct mechanisms. In the lower stratosphere, where ozone has a strong vertical gradient and a long photochemical lifetime and behaves as a material tracer, Kelvin wave vertical advection produces wavelike ozone mixing ratio oscillations (which are in phase with temperature perturbations). In the upper stratosphere, ozone has a short photochemical lifetime and temperature-dependent equilibrium concentration, and temperature fluctuations associated with Kelvin waves are mirrored in local ozone oscillations (which are out of phase with temperature). The transition region in the tropics is near 30–35 km. In this work, we document the signature of Kelvin waves in solar backscatter ultraviolet (SBUV) satellite observations of ozone in the upper stratosphere and use these data to study the variability of Kelvin waves over the years 1979–86.

SBUV data are available from late 1978 into 1987,

* The National Center for Atmospheric Research is sponsored by the National Science Foundation.

Corresponding author address: William J. Randel, NCAR, P.O. Box 3000, Boulder, CO 80307-3000.

and thus permit long-term analyses of ozone variability. In order to validate the Kelvin waves observed by SBUV, we first make comparisons with contemporaneous observations by the Limb Infrared Monitor of the Stratosphere (LIMS) instrument during January–February 1979. LIMS is a limb-viewing sounder with higher vertical resolution than that available with SBUV. These comparisons show that SBUV-derived ozone waves in the tropics are only of sufficient quality in the upper stratosphere (35–55 km), and hence, we focus here on results over that region. The resulting ozone data are spectrally analyzed to isolate eastward-propagating Kelvin wave components. Although the same space–time spectral peaks are found in SBUV and LIMS data, SBUV underestimates the wave amplitudes by approximately 20%–60%. This underestimation is more severe for modes with vertical wavelengths less than 20 km, consistent with the coarser vertical resolution of SBUV measurements. Furthermore, the SBUV data exhibit the curious feature that derived vertical wavelengths are always greater than or equal to 27 km, even for modes that are in reality much shorter. This is possibly related to the inversion algorithm used in the SBUV retrieval.

The continuous eight years of SBUV observations are used to study the seasonal and interannual variability of Kelvin waves, in particular in relation to that of the stratospheric zonal mean zonal wind. The most striking result in these data is a pronounced semiannual modulation of Kelvin wave activity, as first reported by Hirota (1978). We show a seasonal asymmetry in Kelvin wave variance that closely mimics that observed in the upper stratospheric zonal winds. We find a close phase linking between Kelvin wave variance maxima and most intense stratospheric easterlies; there is poor correlation with the mean wind *acceleration*. We interpret this as showing that Kelvin wave absorption is not a dominant mechanism for the westerly acceleration phase of the SAO. An exception to this statement is observed near the stratopause in January when Kelvin wave variance is correlated with positive $\partial\bar{u}/\partial t$; this may suggest that westerly accelerations from Kelvin waves help contribute to the more intense westerlies near the stratopause, which are observed in April.

We also study the interannual variability in Kelvin waves over the eight years of data to search for relationships with the background winds. No consistent association with the quasi-biennial oscillation (QBO) in the lower stratosphere is found. The data hint at a correlation between weak wave variances near the stratopause and upper stratospheric westerlies over the eight Julys, such as would occur if the waves are preferentially absorbed in stronger westerlies, although a similar association is not found during January. The lack of a strong interannual correlation supports the hypothesis that Kelvin wave forcing does not primarily drive the SAO.

2. Data and analyses

a. SBUV data

The SBUV instrument was launched on the *Nimbus-7* spacecraft in October 1978, and obtained reliable data until an instrumental problem developed in early 1987. As the name indicates, SBUV measured the solar ultraviolet radiance backscattered to space at 12 wavelengths between 250 and 340 nm (Heath et al. 1975, 1978). The solar irradiance was also measured on a daily basis, and the ratios of backscattered radiation at each wavelength are input to an optimal statistical estimation algorithm to produce the vertical distribution and total column amounts of ozone (Mateer 1977; Bhartia et al. 1984). An a priori climatological ozone structure and its statistical covariance patterns versus height are used in the estimation scheme. The climatological structure is a function of latitude and season, while the covariance matrix is independent of time and place.

The weighting functions for SBUV peak at altitudes between 25 and 50 km, with full vertical widths at half maximum ranging from 15 to 25 km, and are characterized by large overlap. The information content of the SBUV radiances is discussed in WMO (1991) and summarized in NASA 1208 (1988). Their conclusion is that the SBUV data should be capable of representing the ozone profile from 16 to 0.7 or 0.5 mb (approximately from 28 to 52–56 km). The vertical resolution available from these data is suggested by the scales contained in the "averaging kernels," which show how the retrieved profile is related to the true profile (Rodgers 1990; WMO 1991, see Fig. 3.4). The SBUV averaging kernels over 30–50 km are Gaussian shaped with widths near 8–10 km. This suggests that these measurements should be sensitive to oscillatory features with vertical wavelengths greater than, or equal to, approximately twice this size (i.e., 16–20 km), provided the amplitude is large enough. This sensitivity limit is approximately confirmed in our analyses.

There is the further question of the quality of the data. First, it should be noted that until 1983 the SBUV was turned off for one day in four, because of power limitations, resulting in regularly spaced data gaps. The treatment of these is described in section 2b. The eruption of El Chichón in early 1982 injected large amounts of particulate matter into the stratosphere, which affected the albedo and thus the ozone profiles to some extent, although not catastrophically. Finally, as discussed in NASA 1208 (1988), the diffuser plate that was used to measure the solar irradiance suffered increasing degradation with time. Corrections were applied to alleviate this effect, although the evidence suggests that the corrections did not adequately represent true diffuser change, resulting in a spurious 25% ozone decrease at 1 mb from 1978 to 1986. Fleig et al. (1986) show a slow long-term drift of order −0.5% per year

when SBUV column ozone is compared to the ground-based Dobson network. Because we study zonal-wave components normalized by the background zonal means (see below), such long-term drifts should not affect our results.

The SBUV data are in the form of individual profiles located over the globe. To use them for the following analyses, the profiles near each mapping latitude were treated as a time series and objectively analyzed or mapped using a Kalman filter, as described by Rodgers (1977), to give an estimate of the zonal mean and the amplitudes of the sine and cosine coefficients of the first six waves in the zonal direction. The mapping latitudes include the equator and latitudes spaced every 4 degrees from it. The Kalman filter is run over the data in both forward and reverse time, and the results are combined and weighted by the inverse of their errors to give an optimal estimate for 1200 UTC each day. In the following analyses, the amplitudes and phases of the first two zonal waves ($k = 1, 2$) have been used.

Randel (1990) analyzed the Kelvin wave signatures in LIMS ozone in terms of the ozone mixing ratio μ' at each pressure level. Power spectra for such data have the feature that the middle stratosphere is highlighted over the upper stratosphere (see Randel 1990, his Fig. 3). In the photochemical equilibrium regime above 35 km, ozone–temperature perturbations satisfy

$$\mu' \approx -\left(\frac{\Theta}{\Gamma}\right)T', \tag{1}$$

where Θ and Γ are photochemical parameters discussed in Hartmann and Garcia (1979). Furthermore, to leading order the ratio (Θ/Γ) is proportional to $(\bar{\mu}/\bar{T}^2)$, where overbars denote the background (zonal) means [Hartmann and Garcia 1979, Eq. (A13)]. Hence,

$$(\mu'/\bar{\mu})\alpha\left(\frac{T'}{\bar{T}^2}\right). \tag{2}$$

Because the background structure in the equatorial stratosphere is such that fractional variations of $\bar{\mu}$ are much larger than those for $\bar{T}^2$, power spectra of μ' maximize near large $\bar{\mu}$ (and obscure structure in the upper stratosphere). To alleviate this dependence, we analyze wave components of the ozone field normalized by the background zonal means, i.e., $\mu'/\bar{\mu}$.

b. *Spectral analyses*

Much of this study utilizes space–time cross-spectral analyses to isolate Kelvin waves in SBUV data. As noted above, SBUV data prior to 1984 have a substantial number of days when no measurements were made (approximately 1 out of every 4 days). Because of the high density and regular occurrence of missing data, standard spectral analyses using interpolated values are found to give spurious high-frequency signals. To get around this problem, we utilized a technique that ignores the missing days' data.

Eastward–westward cross-spectral power density at frequency $\pm\omega$ (positive corresponding to westward propagation) for a particular zonal wavenumber is calculated according to the standard formula given by Hayashi (1982):

$$P(\pm\omega) = \tfrac{1}{4}\left[P_\omega(C) + P_\omega(S) \pm 2Q_\omega(C, S)\right]. \tag{3}$$

Here, $P_\omega(C)$ is the power estimate at frequency ω for the zonal-wave cosine coefficient time series, likewise $P_\omega(S)$ for the sine coefficient, and $Q_\omega(C, S)$ is the quadrature spectrum estimate between the cosine and sine time series. These power and cross-spectral estimates were made here by using a lag-correlation spectral analysis as described in standard texts (Chatfield 1980, Chapter 7), i.e., by discrete Fourier transformation of lagged auto- and cross-covariance estimates. The difference here is that the lagged covariance estimates are calculated by considering only the available data (i.e., missing day data are simply disregarded when calculating the lagged auto- and cross correlations). Tests with synthetic time series have shown this technique to give accurate spectral estimates for the amount of missing data encountered here. Time series of length 60 days are analyzed using a maximum lag of 30 days, and a Tukey window is applied by smoothing the spectra with a 0.25–0.50–0.25 convolution in frequency. The resulting spectral bandwidth is $\Delta\omega = [8\pi/(3 \times 30$ days)] (Chatfield 1980, p. 154). Most of the spectra are plotted with a period cut off at 3 days because there is little observed power at 2–3-day periods, and such diagrams allow a better focus on the 5–15-day periods of interest here.

3. Comparison with LIMS data

In this section, a detailed comparison is made of Kelvin wave features observed in LIMS and SBUV ozone data. The LIMS instrument (Gille and Russell 1984) flew during 25 October 1978 to 28 May 1979, a period that overlapped the first operational SBUV results. The most notable difference between the two satellite-based ozone monitors is that LIMS is a limb-viewing instrument, while SBUV is a nadir sounder. LIMS produces a profile with higher vertical resolution than that possible with SBUV; comparison with LIMS thus gives a benchmark with which to validate the SBUV Kelvin waves. Furthermore, LIMS sampled the atmosphere nearly twice as often as SBUV because it was not limited to the sunlit portion of the globe. We note that the zonal means in LIMS and SBUV data are very similar above 5 mb, and differences in nor-

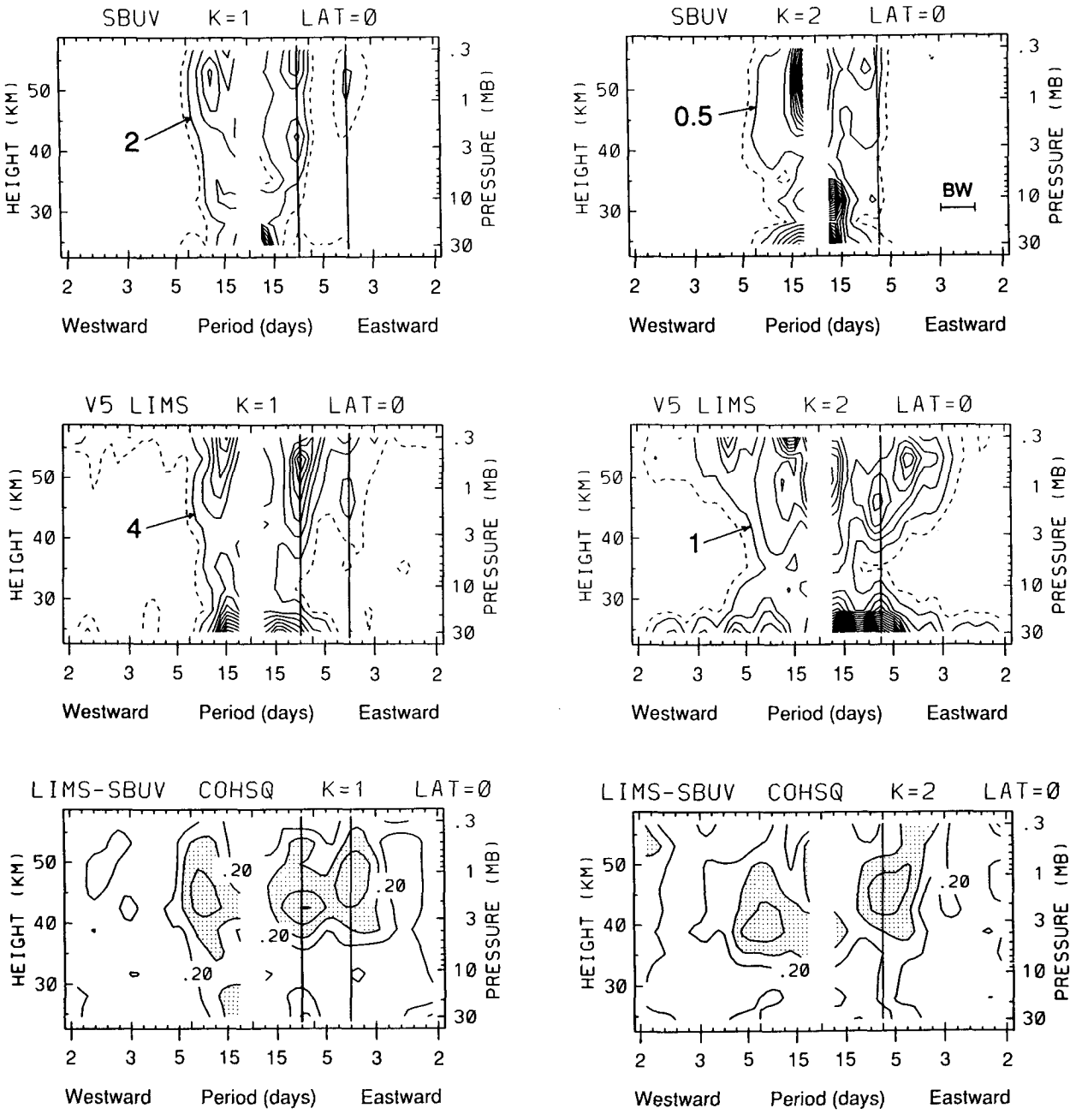

FIG. 1. Top and middle panels show height–frequency cross sections of eastward–westward-propagating spectral power density for equatorial ozone observations, based on SBUV data (top) and LIMS data (middle). Wave components have been normalized by the background zonal means, as discussed in text. Calculations were made for data over January–February 1979. Power density contour intervals are noted in each panel, with units of $10^{-6}\Delta\omega^{-1}$; dashed lines are one-half of the lowest contour level. Left panels are for zonal wave 1, right panels for zonal wave 2; note that the LIMS data contour intervals are twice those of SBUV. Bottom panels show cross sections of coherence squared between LIMS and SBUV data. Contour interval is 0.2, with values above 0.4 stippled. The spectral bandwidth (BW) is indicated in the upper right panel. Vertical lines in each panel denote location of Kelvin waves discussed in text.

malized wave structures are due solely to the waves in the data.

Two sets of daily mapped profiles have been produced from the LIMS radiance measurements, noted version 4 and version 5 (V4 and V5), and significantly different results are found for ozone Kelvin waves between the two (as discussed extensively in Randel 1990). LIMS V5 data are found to be superior to V4

in the lower stratosphere (where Kelvin wave transport is dominant), while both data give qualitatively similar results in the upper stratosphere (where temperature-dependent photochemistry is responsible for ozone Kelvin waves). We use LIMS V5 data here for comparison with SBUV, and extract data on the same ten pressure levels as those analyzed for SBUV. Spectral analyses for these comparisons are calculated over 60 days, 1 January–1 March 1979.

Figure 1 shows spectral power density versus height for the normalized ozone fluctuations of zonal waves 1 and 2 at the equator for both SBUV and LIMS data. The individual coefficients have been averaged over 8°N–8°S to isolate Kelvin waves, which are symmetric about the equator. Spectral maxima corresponding to eastward-propagating Kelvin waves are seen in both sets of data: wave 1 has maxima near 7.5 and 3.8 days, wave 2 near 6 and 4.3 days (the latter maximum not seen in SBUV). Rms temperature amplitudes for the individual Kelvin modes are of the order 1 K; this value is consistent with the ozone wave amplitudes observed in these data—the ratios are calculated explicitly and compared to photochemical model results in Randel (1990). Ozone spectral power is smaller in the SBUV as compared to the LIMS data, particularly for the eastward-propagating wave 2 features (the amplitude differences are discussed further below).

Coherence squared spectra between the two datasets are shown in the lower panels of Fig. 1; these show frequencies–heights for which the two data are statistically coherent (the coherence squared is analogous to the squared correlation coefficient at a particular frequency, i.e., it measures the linearly related variance between the two time series). For the calculations here a coherence squared of 0.44 (0.53) is significant at the 90% (95%) level. The coherence squared spectra in Fig. 1 are very similar for waves 1 and 2: significant values are found primarily over 5–0.5 mb (38–52 km) for the eastward-moving Kelvin waves and low-frequency westward-propagating waves. Very little coherence is seen at and below 7 mb (35 km), which is near the transition level where ozone decouples from the temperature. In relation to the analysis of Kelvin waves in SBUV data, these comparisons suggest that only the upper-stratospheric data are of sufficient quality for further study; transport-induced ozone oscillations in the lower stratosphere are not recoverable in SBUV data.

The vertical phase structures of individual wave modes in the two datasets are compared in Fig. 2. Individual modes are synthesized from the spectra by integrating (summing) the coefficients over a spectral band centered on the chosen frequency. Figure 2 shows the vertical phase structure of several Kelvin waves identified in the power spectra in Fig. 1: eastward-propagating wave 1 at periods of 7.5 and 3.8 days, and eastward-propagating wave 2 at 6.0 days. Also shown for comparison is westward-propagating wave 1 at 10.0 days (representing low-frequency variance presumably forced in the winter extratropics). These vertical phase structures reveal the vertical wavelengths and phase tilts associated with each mode; note the Kelvin waves tilt eastward with height. The approximate vertical wavelengths derived from these plots are also noted in Fig. 2. LIMS data show wavelengths near 19 and 35 km for the 7.5- and 3.8-day wave 1 modes, near 15 km for the wave 2 feature, and $\geq$60 km for the westward-moving wave 1. These former values are in reasonable agreement with the Kelvin wave dispersion relation (see Hitchman and Leovy 1988), and the latter is consistent with an extratropical planetary wave. SBUV-derived vertical phases are in reasonable agreement for the 35- and 60-km features, but differ substantially for the 19- and 15-km waves. In both instances, SBUV data give vertical wavelengths near 27 km. Similar analyses of vertical phase structures from SBUV data during other years reveal that the shortest vertical wavelength ever found is near this 27-km limit and, furthermore, that this value is usually observed for the lowest frequency eastward-moving waves (regardless of the exact central frequency). As the true wavelengths are in reality shorter, this is a bias somehow built into the SBUV data. It may be due to either the broad SBUV weighting functions or the statistical retrieval scheme used to derive profile information (or a combination of the two). Analysis of the weighting function information (discussed in section 2a) suggests that vertical wavelengths of 16–20 km should be resolved, and there is no apparent tie to the 27-km value. One possibility is that the vertical-covariance matrix used in the retrieval limits vertical variations to this value and does not admit higher-frequency variations to the solution; note that the off-diagonal elements of this matrix were estimated subjectively and were likely based primarily on data away from the tropics.

The ratio of ozone wave amplitudes measured by SBUV and LIMS is shown in Fig. 3 for the four wave modes discussed in Fig. 2. Amplitudes are calculated as the square root of twice the spectral power integrated over the specific frequency bands. The amplitude ratios at 3, 2, 1, and 0.5 mb are plotted in Fig. 3 versus the vertical wavelength of the ozone wave, as analyzed in the LIMS data. We choose these pressure levels for comparison because these are the levels over which LIMS–SBUV data are most strongly coherent (Fig. 1). Figure 3 shows amplitude ratios of order 0.4–0.8, with large variability between the different levels for the Kelvin waves. Such differences in detail can also be seen in the power spectra in Fig. 1; for example, the single maximum with height in LIMS data for the 7.5-day wave 1 mode, versus the double-peaked structure in SBUV data (with a minimum near 1 mb). The cause of these differences is unknown, but their presence cautions against overinterpretation of the detailed ver-

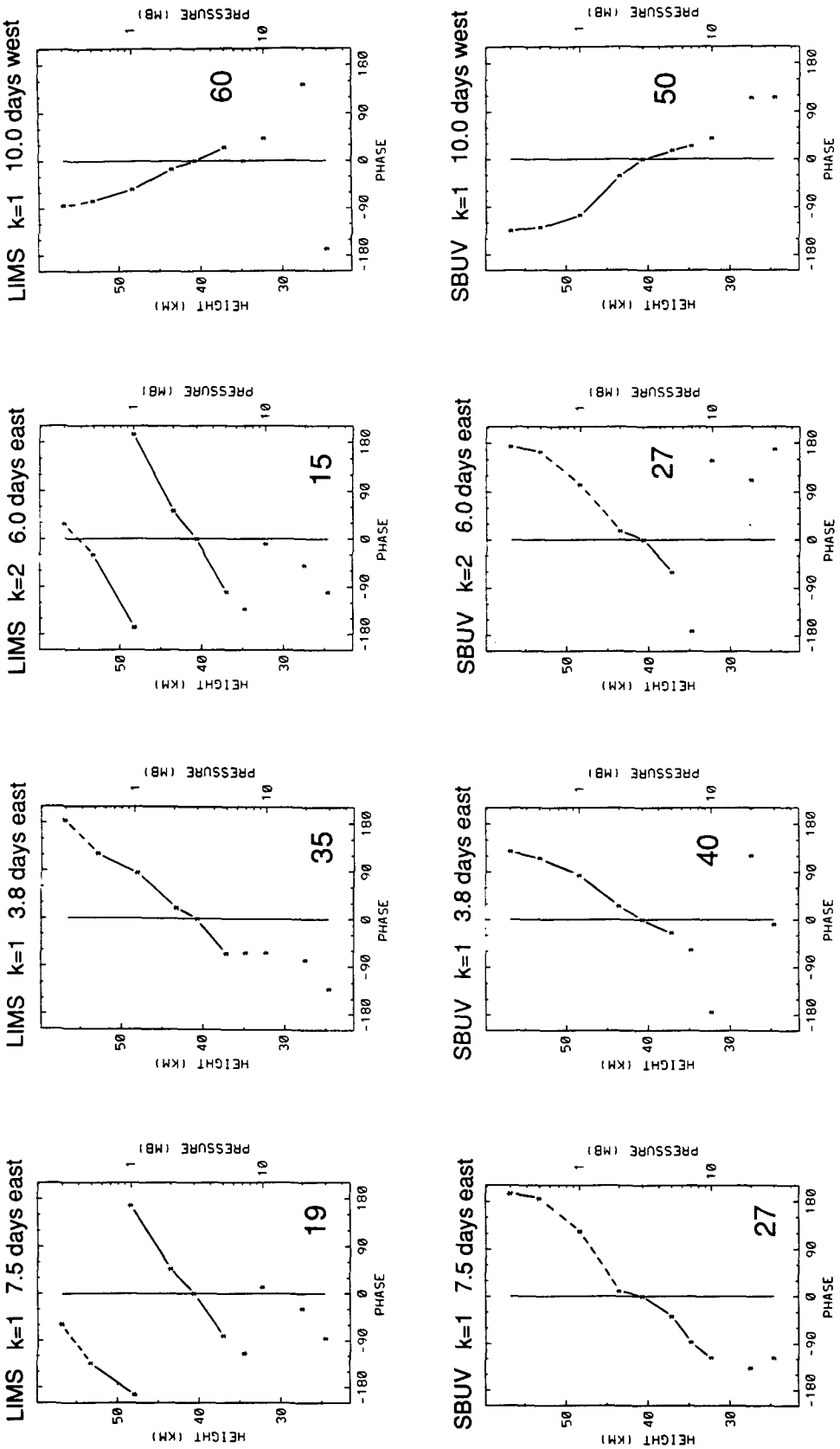

FIG. 2. Vertical phase structure of selected wave modes, identified in Fig. 1, for LIMS data (top) and SBUV data (bottom). Phases are noted with asterisks at each pressure level, and levels that are statistically coherent with the 3-mb reference are connected with solid lines. Numbers in each panel denote the approximate vertical wavelengths in kilometers.

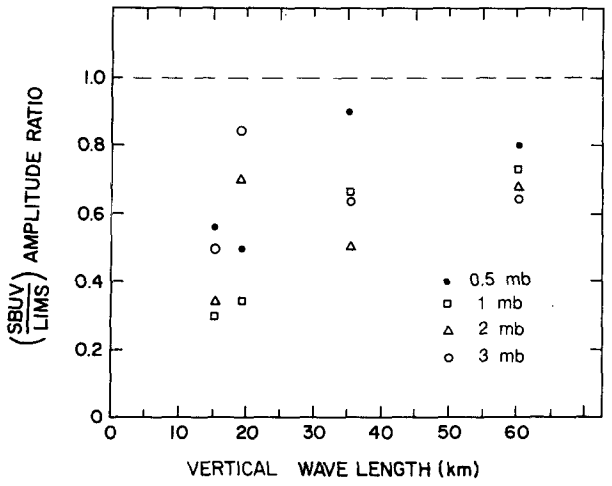

FIG. 3. Amplitude ratio of ozone waves detected by SBUV and LIMS for the modes selected in Figs. 1–2, plotted as a function of their vertical wavelengths as determined from LIMS data. Ratios are shown for the 3-, 2-, 1- and 0.5-mb levels.

tical structures in these data. The ratios in Fig. 3 show an overall decrease as the vertical wavelength decreases. The SBUV data appear sensitive to features with vertical wavelengths ≥ 15 km, with substantially reduced amplitudes for wavelengths near 15 km. This is in good agreement with the analysis of the SBUV weighting functions discussed in section 2a. However, the final profiles appear to be constrained via the retrieval algorithm to have $\lambda_z \geq 27$ km. Table 1 lists periods of zonal wave 1 and 2 Kelvin waves in a realistic background zonal flow $\bar{u} = -20$ m s^{-1}, based on the dispersion relation $\omega = \bar{u}k - Nk/m$ (Andrews et al. 1987), with $N = 2 \times 10^{-2}$ s^{-1}. For a limiting vertical wavelength of 15 km, SBUV can adequately observe zonal wave 1 features with periods shorter than approximately 14 days. Hirota (1978) found that the vertical wavelength of upper stratospheric Kelvin waves is typically $\lambda_z \sim 20$ km (based on rocketsonde data), consistent with the wave 1 periods of order 10 days observed here. Hence, the SBUV data are probably quantitatively accurate for zonal wave 1 features. Because zonal wave 2 features in the same frequency range have vertical wavelengths at or below the 15-km limit, their observations in SBUV data are more problematic, and we focus on the wave 1 results here. Based on the overall comparisons, Kelvin wave variability is analyzed using the 3- and 0.5-mb level data; these are the most widely spaced levels in the vertical (implying independence) for which the data appear reliable.

4. Results

a. Monthly spectra and annual composites

Figure 4 shows eastward–westward-propagating spectral power density at 3 mb for zonal wave 1 at the equator, calculated for each individual month over the years 1979–86. The coefficients were averaged over 8°N–8°S to isolate the component symmetric about the equator. The spectra were calculated from overlapping 60-day time series centered on each month (17 December–15 February were used for the January spectra, etc.). As discussed in section 2, there is a significant fraction of days during 1979–83 when SBUV did not make measurements, and the spectra in Fig. 4 was calculated using only the days when data were available (as described in section 2). Figure 4 includes a line on the right-hand side of the spectra indicating the number of days (out of 60) that data were available and used in the spectral calculations. From mid-1979 until mid-1983, approximately 45 out of every 60 days of data were available; during late 1983 to 1986 there was relatively little missing data.

The spectra in Fig. 4 show episodic maxima for both eastward- and westward-propagating waves. The eastward-moving features are identified as Kelvin waves from their eastward propagation, symmetry about the equator, and eastward vertical phase tilt with height (as shown for the January–February 1979 spectra in Fig. 2 and calculated explicitly for many of the spectral maxima identified in Fig. 4). The Kelvin waves exhibit maxima twice per year, centered near January and July, with the strongest maxima observed in January. Eastward spectral maxima are observed primarily in the 5–15-day period range, with a maximum typically near 8–10 days period (zonal phase speeds near 45–60 m s^{-1}). The central frequency and spectral width of each maximum is variable from year to year. April 1983 shows an isolated event with period near 5 days.

Figure 5 shows a similar spectral diagram for wave 1 at the 0.5-mb level. Similar patterns to that seen at 3 mb are found, and most of the individual spectral maxima seen at 3 mb can also be identified at 0.5 mb. A secondary wave 1 spectral peak at periods of 4–5 days is sometimes observed at 0.5 mb in conjunction with the lower-frequency peak, such as during January 1979, 1984, and 1986. This high-frequency Kelvin wave is observed in some general circulation model (GCM) results, such as those reported in Hayashi et al. (1984), while it is absent in other GCMs (Boville

TABLE 1. Relation between vertical wavelength and wave period for idealized Kelvin waves in background wind $\bar{u} = -20$ m s^{-1}.

	Period (days)	
Vertical wavelength	Zonal wave 1	Zonal wave 2
5	60	30
10	30	15
15	14	7
20	9	4.5
25	7	3.5
30	5.5	2.7
40	4	2

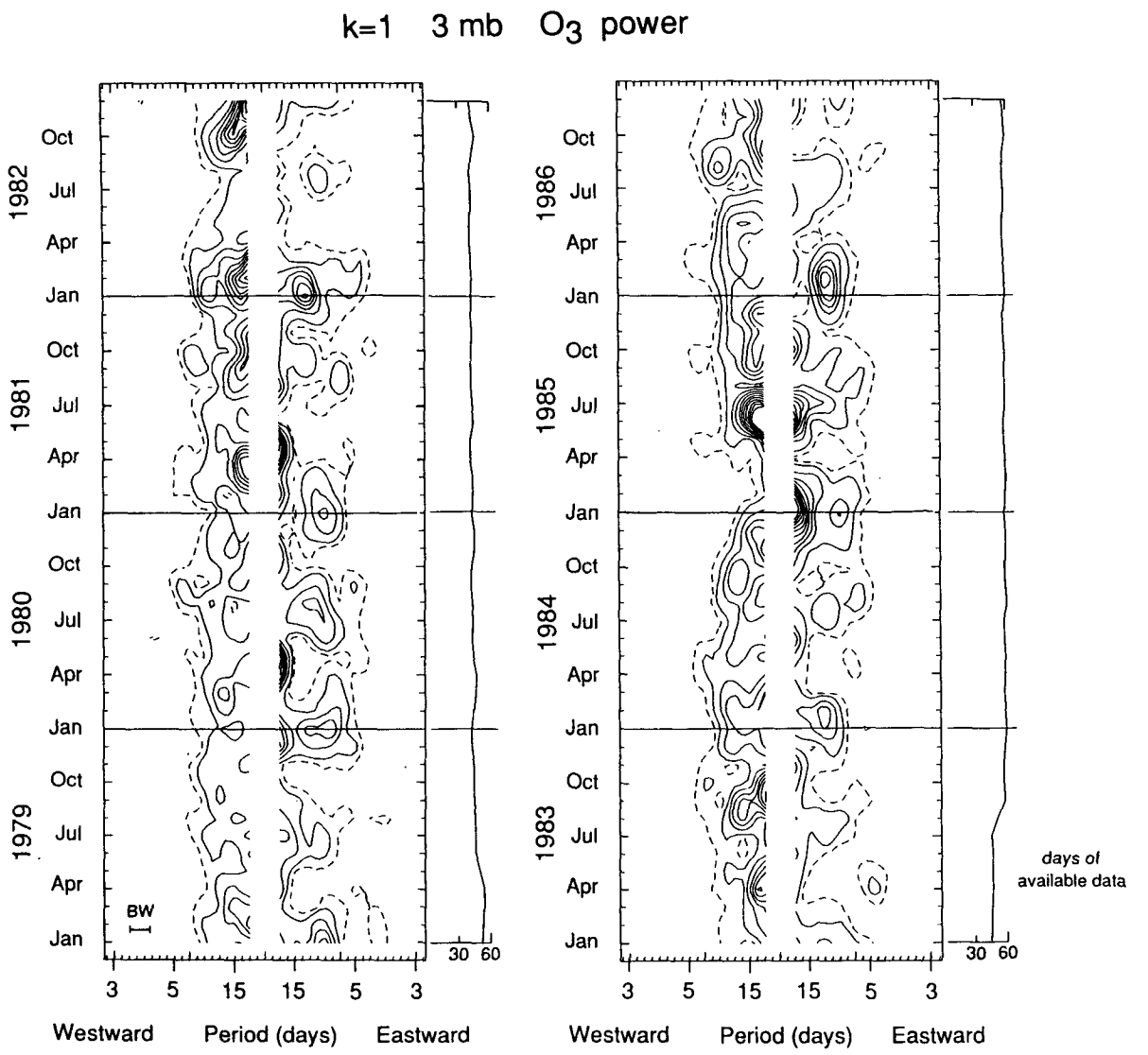

FIG. 4. Eastward–westward-propagating spectral power density for normalized zonal wave 1 ozone fluctuations over the equator for the eight years 1979–86. Spectra are calculated for running 60-day time series centered on each month. Contour interval is 2 $\times 10^{-6}\Delta\omega^{-1}$, and dashed lines are one-half of the lowest contour. The spectral bandwidth (BW) is indicated at lower left. The line on the right-hand side of the plots indicates the number of days (out of 60) when SBUV data were available.

and Randel 1991). The differing GCM results may be related to the respective parameterized convective heating profiles in the upper troposphere and the resulting projection onto different Kelvin modes (e.g., Garcia and Salby 1987). The SBUV data in Fig. 5 suggest that the higher-frequency peak is present only episodically in the atmosphere.

An interesting feature seen in the 0.5-mb spectra is that periods of enhanced eastward-propagating wave activity are often accompanied by bursts of low-frequency westward-moving variance. Clear instances of this are seen in January 1979, 1980, 1982, 1984, and 1986, and July 1982 and 1983 in Fig. 5. Similar features are sometimes found at 3 mb (Fig. 4), as in January 1982 and 1984, but are absent at other times, as in January 1980 and July 1982. The westward-propagating features at 0.5 mb are typically centered at slightly lower frequency than the corresponding eastward spectral peaks. Comparison of the vertical structures of the waves shows that the westward-moving waves have deep vertical structures ($\lambda_z > 50$ km) that tilt westward with height, while the eastward-moving waves tilt eastward with height with shorter vertical wavelengths; see, for example, the phase structures shown in Fig. 2.

The meridional structures of the eastward and westward modes are also completely different. Figure 6 shows wave 1 power spectra versus latitude (over

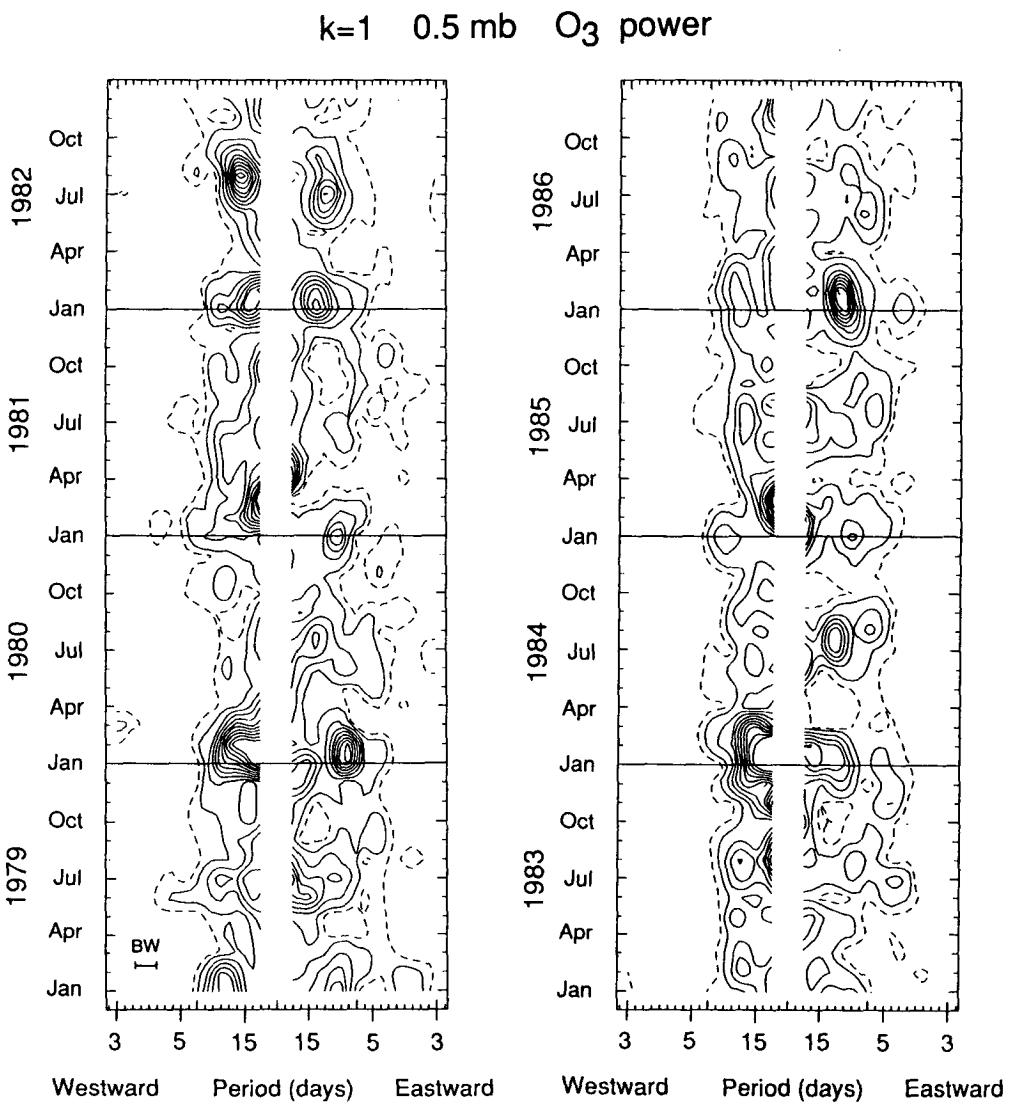

FIG. 5. As in Fig. 4, but for normalized zonal wave 1 ozone fluctuations at 0.5 mb. Contour interval is $2 \times 10^{-6}\Delta\omega^{-1}$.

60°N–60°S) at 0.5 mb for three cases. Here, we have analyzed 90-day time series in order to more clearly resolve low-frequency variability; results are shown in Fig. 6 for December–February 1979 and 1986 and July–September 1982. The eastward-propagating variance in the tropics in all three cases has the equatorially trapped signature of Kelvin modes. The westward variance with periods near 10 days in the tropics has a more global character, with strong maxima in the winter hemisphere. Further analyses, to be reported in detail elsewhere, suggest that the westward-moving waves are associated with global normal mode Rossby waves, such as those identified by Madden (1978), Hirooka and Hirota (1985), and Venne (1989). The observed occurrence of these waves during the solstices (Fig. 5) probably results from strong excitation in the respective winter hemisphere, as opposed to the Kelvin waves, which primarily respond to tropical zonal winds (as discussed below).

Figure 7 shows the composite seasonal variation of zonal wave 1 spectra, averaged over the 8 years 1979–86, for the 3-mb and 0.5-mb levels. Both levels clearly show the two maxima for eastward-propagating Kelvin waves centered near January and July. The January maximum is about twice as large as that in July at 3 mb and 30% larger at 0.5 mb. Westward variance does not exhibit clear seasonality at 3 mb, but shows a twice yearly peak at 0.5 mb very similar to that seen for the eastward-moving waves (as discussed above). Wave 2 spectra (not shown) exhibit patterns qualitatively similar to those seen for wave 1 in Fig. 7, but with greatly reduced magnitudes.

Figure 8 shows the vertical structure of wave 1 spectra for ensemble-averaged January, April, July, and

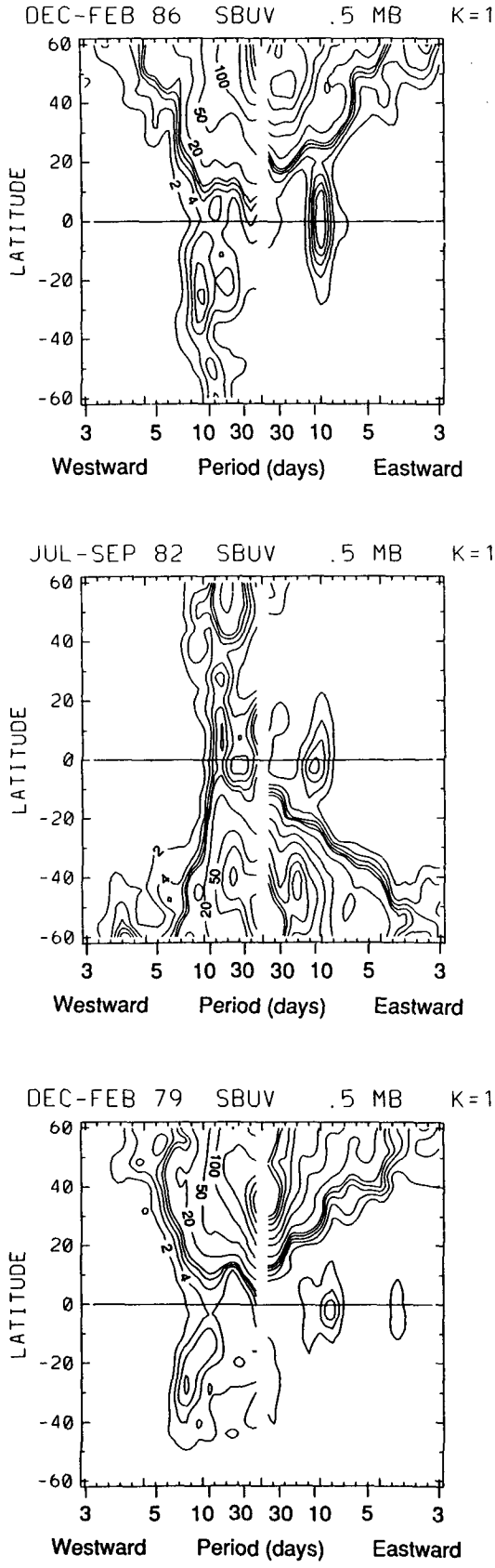

October; the near absence of eastward power is evident in April and October. January spectra show a double maximum in altitude for 8–10-day Kelvin waves, with a relative minimum near 45 km. This structure is not found in LIMS ozone data (Fig. 1), and it is not clear if it is a real feature or due to a pecularity of the SBUV retrieval scheme. July data show only one maximum in altitude. The frequency of the main Kelvin peak at 0.5 mb is slightly faster in January than in July, corresponding to a phase speed difference near 10 m s^{-1}.

Figure 9 illustrates the seasonal variation of Kelvin wave variance for zonal wave 1 at 3 and 0.5 mb. These monthly values are calculated by summing the eastward-propagating spectral power (as shown in Fig. 7) over periods of 5–15 days. Also shown in Fig. 9 are monthly mean zonal mean winds near these two levels, taken from Belmont et al. (1974). Most conspicuous in these figures is the strong Kelvin wave variance observed in association with stratospheric easterlies, as noted previously by Hirota (1978); of further interest here are details observed in these time series. The 3-mb wave variance and 40-km zonal-wind variations show similar asymmetry between January and July, with the stronger wave variances in January associated with more intense easterlies [the asymmetric nature of the semiannual zonal wind oscillation in the stratosphere has been discussed recently by Dunkerton and Delisi (1988)]. This similar evolution is consistent with the interpretation that the Kelvin wave variance in the middle stratosphere is primarily determined by the strength of the zonal winds, due to small attenuation during vertical propagation in easterlies. Note that maxima in wave variances at 3 mb coincide with near-zero values of wind acceleration (the time derivative of the $\bar{u}$ curve can be taken visually in Fig. 9), supporting the hypothesis that Kelvin waves are not the decisive factor for the westerly acceleration phase of the SAO. Note that this is not the case for Kelvin wave variance at 50 mb in relation to the QBO winds: Angel et al. (1973, their Figs. 4–5) show a strong correlation between wave variance and $\partial\bar{u}/\partial t > 0$ at 50 mb, consistent with a dominant role for Kelvin waves in the QBO.

The 0.5-mb Kelvin wave variance in Fig. 9 shows a smaller difference between maxima in January and July than that seen at 3 mb. Likewise, there is a smaller difference in the maximum easterly zonal wind at this level than found lower (at 55 km, the seasonal asymmetry is seen in the strength of the westerlies). The July wave variance maximum at 0.5 mb coincides with easterly wind maximum at 55 km, but the January maximum lags by approximately one month the De-

FIG. 6. Latitudinal sections of the normalized SBUV zonal wave 1 power spectra at 0.5 mb for data over the periods indicated at the top of each panel. Contour levels are 2, 4, 6, 8, 10, 20, 50, 100, 200 . . . , $\times 10^{-6}\Delta\omega^{-1}$. Note the distinctive meridional structures of eastward- versus westward-propagating waves with periods near 10 days.

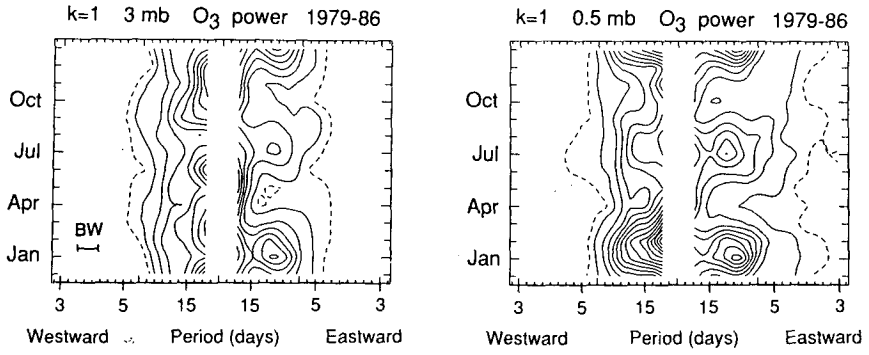

FIG. 7. Eight-year-average ensemble power spectra for normalized zonal wave 1 ozone fluctuations over the equator at 3 mb (left) and 0.5 mb (right). Contour interval is $1 \times 10^{-6}\Delta\omega^{-1}$.

cember easterly wind maximum. This means that the January (and February) Kelvin wave variance maximum occurs coincidentally with strong positive zonal-wind accelerations near the stratopause, suggesting the possibility that the Kelvin waves are contributing to that acceleration. This possible importance of Kelvin-wave–induced accelerations near the stratopause during January (but not July) is furthermore consistent with:

1) the larger-amplitude Kelvin waves found in January (primarily in the middle stratosphere), and
2) the substantially stronger westerlies observed in April as opposed to October at 55 km.

b. Interannual variabilities

In this section, interannual variability of Kelvin wave variances is compared with that of the zonal mean zonal wind in the upper stratosphere. Kelvin wave variances are estimated by integrating the spectral power in Figs. 4–5 over eastward-moving waves with periods of 5–15 days (as in Fig. 8), and averaging over the months December–February (DJF) and June–August (JJA). We analyze DJF and JJA separately in the expectation that there may be differences between the two phases of the SAO, and to test any observed correlations with the QBO for consistency over the short 8-year sample.

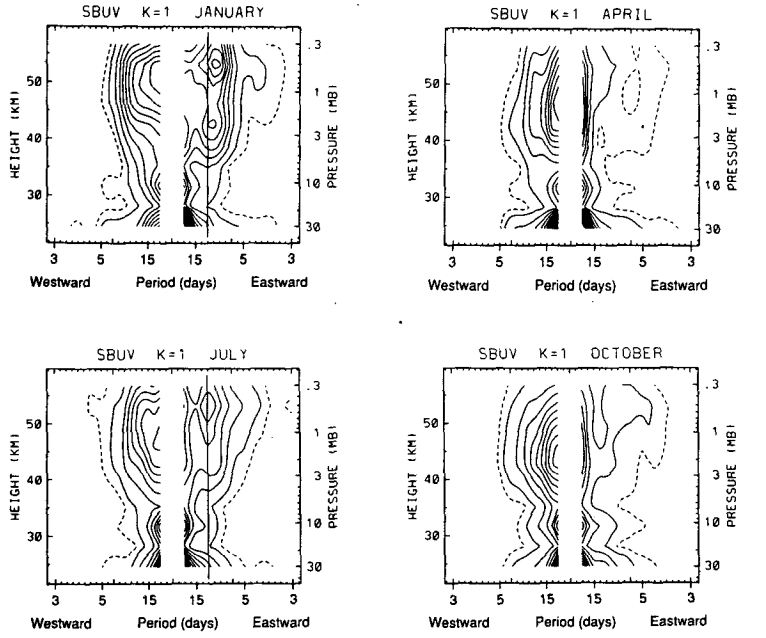

FIG. 8. Ensemble eight-year-average height–frequency sections of normalized zonal wave 1 spectral power for January, April, July, and October. Contour interval is $1 \times 10^{-6}\Delta\omega^{-1}$. The straight lines in January and July denote an eastward period of 10 days.

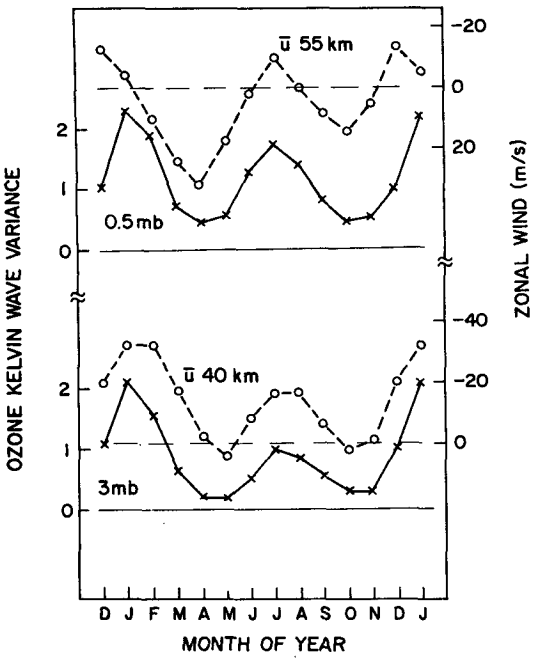

FIG. 9. Seasonal variation of Kelvin wave ozone variance at 0.5 and 3 mb, calculated by integrating the zonal wave 1 ensemble spectra shown in Fig. 7 over eastward-propagating periods of 5–15 days; units are arbitrary. Also shown are zonal mean zonal winds at the 40- and 55-km levels, taken from Belmont et al. (1974). Note that the absisca is inverted for the wind plots.

Three-month–average zonal mean zonal winds in the upper stratosphere are estimated from monthly mean geopotential height data obtained from the National Meteorological Center–Climate Analysis Center (NMC–CAC) via geostrophic balance. Fleming and Chandra (1989) have shown reasonable qualitative agreement between such data and monthly mean tropical radiosonde–rocketsonde measurements. We have compared these wind estimates with those presented in Hitchman and Leovy (1986) for DJF 78–79, calculated from LIMS data, and find good agreement. These data should give good qualitative measures of interannual zonal-wind anomalies in the upper stratosphere. Additionally, the phase of the quasi-biennial oscillation (QBO) in the lower stratosphere at 50–30 mb is tabulated from three-month–average zonal winds obtained from an updated climatology as presented in Naujokat (1986). The QBO propagates downward in time in an irregular manner, and the index at 50 mb is different from that at 30 mb. Kelvin waves likely are most sensitive to the zonal wind in the lower stratosphere averaged over a deep layer. Accordingly, we have used a QBO index that is east or west only if the winds are of the same sign at 50 and 30 mb for all three months of the average; if a transition occurs at any level or month, no value is assigned.

Figure 10 shows plots of 3-mb and 0.5-mb Kelvin wave variances and 1-mb zonal-wind values for DJF, and Fig. 11 shows similar data for JJA. Kelvin wave variances show a substantial degree of variability at each level, with up to a factor of three difference between individual years. The time series do not show identical variability at 3 and 0.5 mb; for example, the 0.5-mb data show relative maxima during DJF 1984 and 1986 (Fig. 10) and JJA 1982 and 1984 (Fig. 11) that are not observed at 3 mb. We have also studied more highly derived diagnostics, such as vertical differences or ratios between SBUV data at different levels, but in light of the differences in vertical structure found between SBUV and LIMS data (see Fig. 1), we do not believe such diagnostics are warranted.

Comparison of Kelvin wave variances with the QBO shows little consistent relationship between DJF and JJA. The strong DJF 1982 3-mb variance maximum (Fig. 10) occurs with the QBO in easterly phase, as would be consistent with the waves being able to propagate to greater heights in the presence of lower stratospheric easterlies. However, the JJA 1980 3-mb variance maximum (Fig. 11) occurs in QBO westerlies, and the QBO easterlies of 1979 and 1984 are not wave maxima. It is likely that variations in the strength at tropospheric wave forcing is also an important factor for Kelvin wave amplitudes in the stratosphere.

Comparison of Kelvin wave variances with the 1-mb zonal winds shows little correlation during DJF

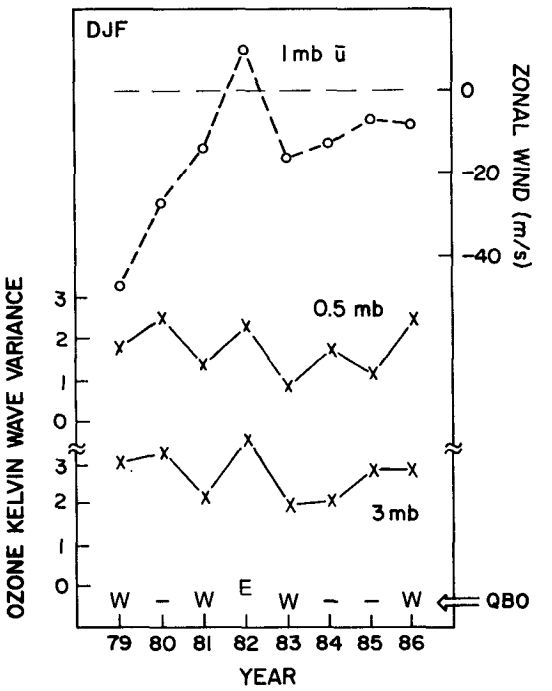

FIG. 10. Interannual variability of Kelvin wave variance at 0.5 and 3 mb (solid lines, calculated as in Fig. 9, units are arbitrary), along with the zonal mean zonal wind at 1 mb (dashed), all averaged over December–February. Also noted at the bottom is the phase of the QBO over 50–30 mb; if a transition occurs within these levels during December–February, no phase is indicated (—).

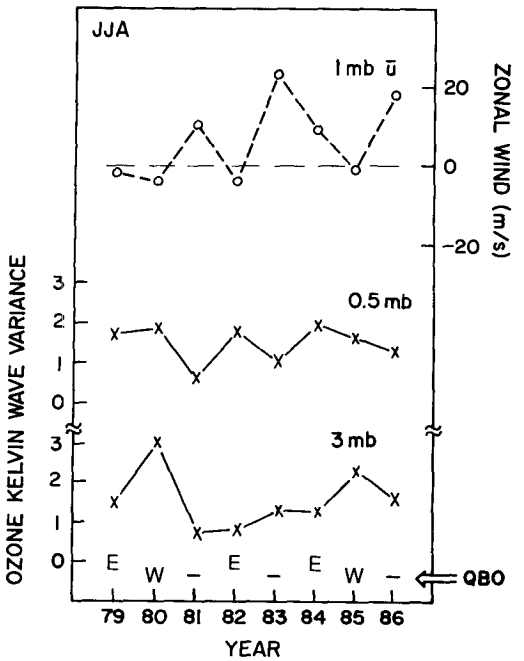

FIG. 11. As in Fig. 10, but for averages over June–August.

(Fig. 10), beyond the observation that the strong 3-mb maximum during DJF 1982 is associated with the only pronounced westerly wind anomaly. This relationship would be consistent with the Kelvin waves forcing westerly zonal accelerations. During JJA (Fig. 11), there is some evidence of anticorrelation between 0.5-mb wave variance and 1-mb zonal wind (i.e., westerlies are associated with relative minima in wave activity). This relationship is consistent with the waves propagating vertically more easily during years with stronger easterly winds. However, the lack of consistent behavior in DJF, together with the rather short time sample, cautions against too strong of an interpretation. The lack of strong positive correlations between wave variance and zonal winds (zonal-wind accelerations were also tested and found uncorrelated) supports the contention that Kelvin waves are not a deciding factor in forcing the SAO.

5. Summary

The higher vertical resolution, larger altitude range, and doubled number of profiles on a given day (day and night) mean that the LIMS data have the capability to follow these tropical waves with greater fidelity than the SBUV data, and thus serve as a useful standard with which to validate the SBUV data. The comparisons show that SBUV data resolve the same eastward and westward-propagating planetary waves 1 and 2, with periods of 5–15 days. Kelvin waves observed in the two datasets are statistically coherent over approximately 3–0.5 mb (40–55 km). However, the derived SBUV wave amplitudes are smaller than those determined by the LIMS data (with ratios of order 0.4–0.8), consistent with SBUV's coarser vertical resolution, and SBUV amplitudes fall off rapidly for waves with vertical wavelengths less than approximately 20 km. Detailed vertical structures over 3–0.5 mb are somewhat different between the two data. Furthermore, the vertical wavelengths of features in SBUV data are found to always be $\geq$27 km, likely due to constraints built into the statistical inversion algorithm.

Analyses of the continuous eight years of SBUV data show that Kelvin waves 1 and 2 in the upper stratosphere and lower mesosphere have two maxima per year, consistently stronger in January than July. The largest variance occurs when zonal mean winds are easterly, suggesting that the amplitudes respond to the conditions that control wave propagation. These waves appear to be in quadrature with the zonal-wind acceleration at 3 mb and nearly so at 0.5 mb, suggesting that Kelvin waves are not a dominant source of momentum for the westerly phase of the SAO. An exception is found at the stratopause during northern winter when strong wave variance coincides with positive $\partial\bar{u}/\partial t$. The influence of Kelvin waves at this time may contribute to the stronger stratopause westerlies observed during NH spring.

Hitchman and Leovy (1988) have estimated the Kelvin wave contribution to the westerly acceleration phase of the SAO during northern winter 1978/79. Their calculations suggest that Kelvin waves contribute 20%–70% of the observed accelerations during this period, with the remainder due to internal gravity waves. Although we cannot directly estimate wave driving from ozone observations, the possible contribution of Kelvin waves at the stratopause during northern winter inferred here is not inconsistent with Hitchman and Leovy's estimates. As a note, Hitchman and Leovy (1988) calculate a parameterized gravity wave drag that is strongly dependent on the mean flow $\bar{u}$; Fig. 10 shows that DJF 1978/79 had anomalously strong easterlies, which could substantially affect their gravity wave calculations (and conclusions regarding the relative importance of Kelvin waves). Our data do suggest a minor role for Kelvin waves at other locations. Consistent with this inference, Hamilton and Mahlman (1988) find that Kelvin waves contribute only minor wave-driving compared to that of gravity waves in forcing the SAO in the GFDL "skihi" general circulation model.

These data also show bursts of westward-propagating waves at 0.5 mb, coincident with the modulated Kelvin wave activity. These westward waves are not always clearly seen at 3 mb. The westward-propagating waves have vertical phase and meridional amplitude structures that are distinctive from the Kelvin waves. Their space–time characteristics suggest they may be related to global normal mode Rossby waves, and we will report on the details of these modes elsewhere. The observed occurrence of the westward-moving waves during the solstices (e.g., Figs. 5–7) is likely related to

strong excitation in the respective winter hemisphere; in contrast, the solstical Kelvin wave maxima occur in response to the tropical zonal winds.

Interannual correlations of Kelvin wave variance in the upper stratosphere with lower stratospheric QBO winds show no consistent associations. Although there is a tendency for an alternation of high and low values of wave variance from year to year, especially at 0.5 mb, there is not a consistent relationship with the zonal winds or their accelerations. This lack of interannual correlation is surprising in light of the strong seasonal coupling observed in these data. The lack of strong correlation is consistent with the proposed minor role of Kelvin waves in forcing the mean flow. In the case where Kelvin waves control the mean flow evolution, one would anticipate that factor of 2 variations in Kelvin wave variance (as observed in Figs. 10–11) would be mirrored in zonal wind changes; this is not observed here.

Acknowledgments. The authors acknowledge many fruitful discussions with Paul Bailey and Eric Fetzer, and helpful reviews by Matt Hitchman, Rolando Garcia, and Roland Madden. Dan Packman provided expertise on the data mapping, and Marilena Stone prepared the manuscript. This work has been supported under NASA Grant W16215.

REFERENCES

Andrews, D. G., J. R. Holton and C. B. Leovy, 1987: *Middle Atmosphere Dynamics.* Academic Press, 489 pp.

Angel, J. K., G. F. Cotton and J. Korshover, 1973: A climatological analysis of oscillations of Kelvin wave period at 50 mb. *J. Atmos. Sci.*, **30,** 13–24.

Belmont, A. D., D. G. Dartt and G. D. Nastrom, 1975: Variations of stratospheric zonal winds, 20–65 km, 1961–1971. *J. Appl. Meteor.*, **14,** 585–594.

Bhartia, P. K., K. F. Klenk, A. J. Fleig, C. G. Wellemeyer and D. Gordon, 1984: Intercomparison of NIMBUS 7 solar backscatter ultraviolet ozone profiles with rocket, balloon, and Umkehr profiles. *J. Geophys. Res.*, **89,** 5227–5238.

Boville, B. A., and W. J. Randel, 1991: Equatorial waves in a stratospheric GCM: Effects of vertical resolution. *J. Atmos. Sci.*, in press.

Chatfield, C., 1980: *The Analysis of Time Series: An Introduction.* Chapman and Hall, 268 pp.

Dunkerton, T. J., 1979: On the role of the Kelvin wave in the westerly phase of the semiannual zonal wind oscillation. *J. Atmos. Sci.*, **36,** 32–41.

——, and D. P. Delisi, 1988: Seasonal variation of the semiannual oscillation. *J. Atmos. Sci.*, **45,** 2772–2787.

Fleig, A. J., P. K. Bhartia and D. S. Silberstein, 1986: An assessment of the long-term drift in SBUV total ozone data, based on comparison with the Dobson network. *Geophys. Res. Lett.*, **13,** 1359–1362.

Fleming, E. L., and S. Chandra, 1989: Equatorial zonal wind in the middle atmosphere derived from geopotential height and temperature data. *J. Atmos. Sci.*, **46,** 860–866.

Garcia, R. R., and M. L. Salby, 1987: Transient response to localized episodic heating in the tropics. Part II: Far field behavior. *J. Atmos. Sci.*, **44,** 499–530.

Gille, J. C., and J. M. Russell III, 1984: The Limb Infrared Monitor of the Stratosphere: Experiment description, performance and results. *J. Geophys. Res.*, **89,** 5125–5140.

Hamilton, K., and J. D. Mahlman, 1988: General circulation model simulation of the semiannual oscillation of the tropical middle atmosphere. *J. Atmos. Sci.*, **45,** 3212–3235.

Hartmann, D. L., and R. R. Garcia, 1979: A mechanistic model of ozone transport by planetary waves in the stratosphere. *J. Atmos. Sci.*, **36,** 350–364.

Hayashi, Y., 1982: Space–time spectral analysis and its application to atmospheric waves. *J. Meteor. Soc. Japan,* **60,** 156–171.

——, D. G. Golder and J. D. Mahlman, 1984: Stratospheric and mesospheric Kelvin waves simulated by the GFDL 'SKYHI' general circulation model. *J. Atmos. Sci.*, **41,** 1971–1984.

Heath, D. F., A. J. Krueger, H. R. Roeder and B. D. Henderson, 1975: The solar backscatter ultraviolet and total ozone mapping spectrometer (SBUV/TOMS) for Nimbus. *G. Opt. Eng.*, **14,** 323–331.

Heath, D. J., A. J. Krueger and H. Park, 1978: The solar backscatter ultraviolet (SBUV) and total ozone mapping spectrometer (TOMS) experiment. The Nimbus 7 Users' Guide. 175–211.

Hirota, I., 1978: Equatorial waves in the upper stratosphere and mesosphere in relation to the semiannual oscillation of the zonal wind. *J. Atmos. Sci.*, **35,** 714–722.

——, 1979: Kelvin waves in the equatorial middle atmosphere observed by the Nimbus 5 SCR. *J. Atmos. Sci.*, **36,** 217–222.

Hirooka, T., and I. Hirota, 1985: Normal mode Rossby waves observed in the upper stratosphere. Part II: second antisymmetric and symmetric modes of zonal wavenumbers 1 and 2. *J. Atmos. Sci.*, **42,** 536–548.

Hitchman, M. H., and C. B. Leovy, 1986: Evolution of the zonal mean state in the equatorial middle atmosphere during October 1978–May 1979. *J. Atmos. Sci.*, **43,** 3159–3176.

——, and ——, 1988: Estimation of the Kelvin wave contribution to the semiannual oscillation. *J. Atmos. Sci.*, **45,** 1462–1475.

Holton, J. R., and R. S. Lindzen, 1972: An updated theory for the quasi-biennial oscillation of the tropical stratosphere. *J. Atmos. Sci.*, **29,** 1076–1080.

Madden, R. A., 1978: Further evidence of traveling planetary waves. *J. Atmos. Sci.*, **35,** 1605–1618.

Mateer, C. L., 1977: Experience with the inversion of Nimbus-4 BUV measurements to retrieve the ozone profile. *Inversion Methods in Atmospheric Remote Sensing.* A. Deepak, Ed., Academic, 557–597.

NASA 1208, 1988: Present state of knowledge of the upper atmosphere 1988: An assessment report. NASA Reference Publication 1208, NASA Scientific and Technical Information Division.

Naujokat, B., 1986: An update of the observed quasi-biennial oscillation of the stratospheric winds over the tropics. *J. Atmos. Sci.*, **43,** 1873–1877.

Randel, W. J., 1990: Kelvin wave induced trace constituent oscillations in the equatorial stratosphere. *J. Geophys. Res.*, **95,** 18 641–18 652.

Rodgers, C. D., 1977: Statistical principles of inversion theory. *Inversion Methods in Atmospheric Remote Sensing,* A. Deepak, Ed., Academic, 117–138.

——, 1990: Characterization and error analysis of profiles retrieved from remote sounding measurements. *J. Geophys. Res.*, **95,** 5587–5595.

Salby, M. L., D. L. Hartmann, P. L. Bailey, and J. C. Gille, 1984: Evidence of equatorial Kelvin modes in Nimbus-7 LIMS. *J. Atmos. Sci.*, **41,** 220–235.

Venne, D. L., 1989: Normal-mode Rossby waves observed in the wavenumber 1–5 geopotential fields of the stratosphere and troposphere. *J. Atmos. Sci.*, **46,** 1042–1056.

Wallace, J. M., and V. E. Kousky, 1968: Observational evidence of Kelvin waves in the tropical stratosphere. *J. Atmos. Sci.*, **25,** 900–907.

World Meteorological Organization (WMO), 1991: Report of the International Ozone Trends Panel—1988. WMO Rep. No. 18, World Meteorological Organization, Geneva, 825 pp.